Effect of oxidation degree of iron-based oxygen carriers on their mechanical strength

Downloaded from: https://research.chalmers.se, 2026-04-06 08:32 UTC

Citation for the original published paper (version of record):
Purnomo, V., Faust, R., Ejjeta, L. et al (2024). Effect of oxidation degree of iron-based oxygen carriers on their mechanical strength. Powder Technology, 438.
http://dx.doi.org/10.1016/j.powtec.2024.119598

N.B. When citing this work, cite the original published paper.

research.chalmers.se offers the possibility of retrieving research publications produced at Chalmers University of Technology. It covers all kind of research output: articles, dissertations, conference papers, reports etc. since 2004. research.chalmers.se is administrated and maintained by Chalmers Library

(article starts on next page)

Powder Technology 438 (2024) 119598

Contents lists available at ScienceDirect

Powder Technology

journal homepage: www.journals.elsevier.com/powder-technology

Effect of oxidation degree of iron-based oxygen carriers on their mechanical strength

Victor Purnomo [a,*], Robin Faust [a], Lidiya Abdisa Ejjeta [a], Tobias Mattisson [b], Henrik Leion [a]

[a] Division of Energy and Materials, Department of Chemistry and Chemical Engineering, Chalmers University of Technology, Göteborg 412 58, Sweden
[b] Division of Energy Technology, Department of Space, Earth, and Environment, Chalmers University of Technology, Göteborg 412 58, Sweden

HIGHLIGHTS

- Oxidation level of an iron-based oxygen carrier may affect its mechanical strength.
- Attrition rate is an important parameter with respect to mechanical strength.
- Porosity of oxygen carriers likely determines its attrition resistance.
- Ilmenite ore and iron sand have shown robust mechanical strength.
- Synthetic ilmenite shows the lowest attrition resistance among all the materials.

GRAPHICAL ABSTRACT

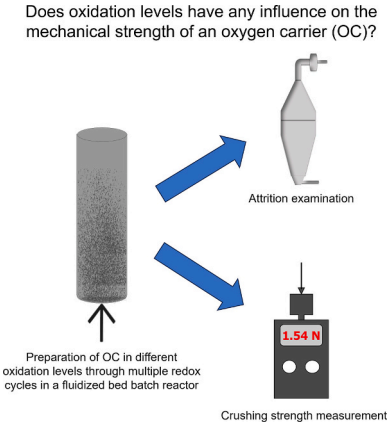

ARTICLE INFO

Keywords:
Oxygen carrier
Attrition resistance
Crushing strength
Mechanical strength
Oxidation degree
Chemical looping

ABSTRACT

Iron-based oxygen carriers are currently one of the most popular choices for chemical looping processes. In order to minimize losses of oxygen carrier materials in the system, it is important to assess attrition characteristics. Furthermore, in chemical looping gasification where the oxygen transfer capacity needs to be limited, a higher reduction degree of oxygen carriers can be expected. As different oxidation degrees lead to different phase compositions, this study aimed to investigate the correlation between mechanical strength of iron-based oxygen carriers and the phase composition, which is the result of oxidation degree change. Our findings demonstrate that how the phase composition may affect the attrition rate of oxygen carriers depends largely on the type of the

Abbreviation: A, Attrition rate based on investigation in the customized jet cup device; AJI, Air jet index; AR, Air reactor; A_{tot}, Initial attrition rate observed during the whole hour of observation; A_{30-60}, Attrition rate observed during the last 30 min into observation; CFD, Computational fluid dynamics; CLC, Chemical looping combustion; CLG, Chemical looping gasification; CLR, Chemical looping reforming; CLWS, Chemical looping water splitting; EDX, Energy-dispersive X-ray spectroscopy; FC, Freshly calcined; FCC, Fluid catalytic cracking; FO, Fully oxidized; FR, Fuel reactor; LD, Linz – Donawitz; M_O, molecular weight of oxygen; MR, moderately reduced; m_{ox} , mass of oxygen carrier at its fully oxidized state; $\dot{n}$, outlet molar flow; OC, oxygen carrier; OCAC, Oxygen carrier aided combustion; t, reaction/observation time; SEM, Scanning electron microscopy; SR, substantially reduced; x_i, molar fraction of species i; XRD, X-ray diffraction; ω_i, mass conversion degree of an oxygen carrier in converting species i.

* Corresponding author.
E-mail address: purnomo@chalmers.se (V. Purnomo).

https://doi.org/10.1016/j.powtec.2024.119598
Received 13 October 2023; Received in revised form 16 January 2024; Accepted 3 March 2024
Available online 7 March 2024
0032-5910/© 2024 The Authors. Published by Elsevier B.V. This is an open access article under the CC BY license (http://creativecommons.org/licenses/by/4.0/).

material itself. In this study, the presence of Fe-Ti and Fe-Si combinations contribute to a generally stable attrition rate, while Fe-Ca system exhibits a decreasing attrition rate. Furthermore, attrition rate shows a more conclusive trend compared to crushing strength. Among the investigated materials, both ilmenite ore and iron sand showed a robust, stable mechanical stability with an attrition rate of approximately 0.5–1 wt%/h, which is on par with that of sand (0.5 wt%/h). The attrition rates of LD slag and mill scale are lower, about 1–3 wt%/h.

1. Introduction

Having been studied extensively for around three decades, oxygen carriers are crucial to the development of energy conversion processes like chemical looping technology and oxygen carrier aided combustion (OCAC) [1]. While the use of oxygen carrier in OCAC increases the combustion efficiency and heat distribution in the boiler, it has an even more essential role in chemical looping technology. Apart from the mentioned benefits, an oxygen carrier is responsible for transferring oxygen from the air to the fuel reactor through redox cycles in a chemical looping unit. This virtually eliminates the presence of nitrogen in the product gases and, therefore, also the need for an energy-extensive gas separation step. This is why an efficient carbon dioxide capture is possible through the establishment of a chemical looping unit.

There are several processes which use oxygen carriers for different purposes. In chemical looping combustion (CLC) and OCAC, a high oxygen transfer capacity is desired to fully combust the fuel, generating carbon dioxide and steam as the main gaseous products. However, this is not always the case with other processes such as chemical looping gasification (CLG), chemical looping reforming (CLR), or chemical looping water splitting (CLWS). The expected main products of these processes are syngas, i.e., carbon monoxide and hydrogen, or only hydrogen in the case of CLWS. These products are highly valuable as precursors to various chemicals. Contrary to CLC and OCAC, complete fuel combustion is not expected in these processes, although some CO_2 will necessarily be generated in the fuel reactor together with the syngas in order to achieve autothermal process [2]. As an illustration, Fig. 1 demonstrates schematic setups of CLC and CLG.

The main challenge of processes like CLG, where partial fuel conversion takes place, is maintaining a sufficient oxygen transfer from the air reactor (AR) to fuel reactor (FR) in order to establish a successful gasification reaction. This may result in a higher reduction degree of the oxygen carrier, which may lead to several issues like particle agglomeration, reactivity decrease and compromised mechanical strength [3]. Adánez et al. [4] suggested that mechanical strength is one of the most important parameters in oxygen carrier screening. The mechanical strength of an oxygen carrier can be evaluated in different manners, e.g., by measuring its attrition resistance and crushing strength. Attrition resistance evaluation is applicable for utilization of oxygen carriers in fluidized bed reactors since this characteristic strongly influences particle elutriation and size distribution [5]. On the other hand, crushing strength represents the maximum compressive load the particles can withstand without experiencing breakage, which is determined by composition and morphology of the particles [6]. Understanding the crushing strength of oxygen carriers can be useful for predicting their stress and strain behaviors [7], which are important factors in a fluidized bed setup where particles are exposed to mechanical stress [8].

Previous studies have successfully established the concept of attrition on particles in a fluidized bed setup and examined the attrition resistance of various oxygen carrier materials. The main causes of attrition have been identified as mechanical, thermal, and chemical stresses [9,10]. Different types and sources of attrition in a fluidized bed energy conversion setup have also been elaborated [11]. Further, there are several known methods to determine the attrition resistance of particles. The simplest one is to attach a dust filter to the outlet of a fluidized bed setup to collect the fragments from the fluidization, so that

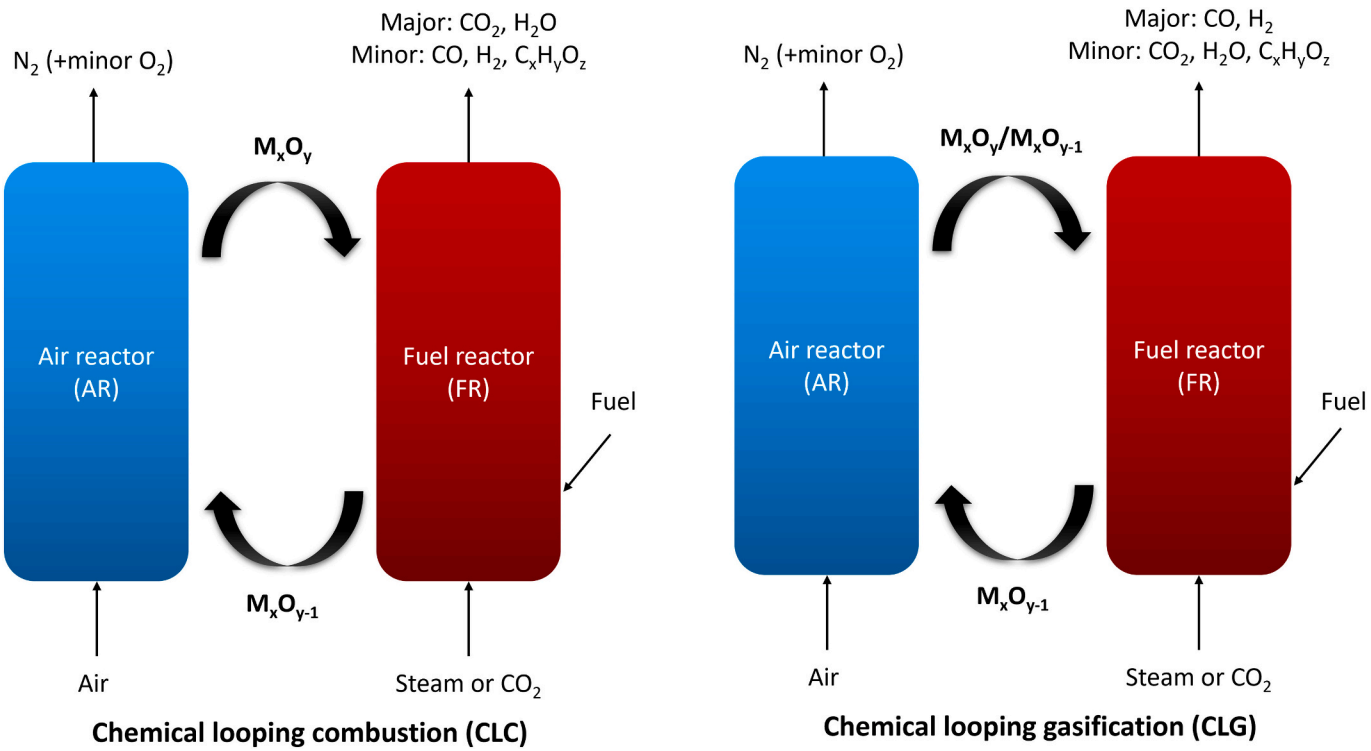

Fig. 1. Illustrative diagrams of chemical looping combustion and gasification.

the attrition rate can be determined directly after a certain period based on the weight of the collected fines. For instance, Miccio et al. [12] also examined the attrition rate of several synthetic geopolymer-based iron materials directly in a lab-scale fluidized bed equipped with a dust trapping filter for 24 h. They found that the geopolymer materials show excellent attrition resistance, about three times lower than the elutriation rate of ilmenite in a chemical looping unit reported by Cuadrat et al. [13].

Another well-known strategy is to examine the attrition rate of particles in a jet cup rig. This device works well to estimate the attrition tendency of oxygen carriers caused by mechanical stress due to the collision between the particles and jet cup wall [14]. However, it is not possible to directly consider the effects of thermal stress, let alone chemical stress, in a jet cup rig. The established standard method ASTM D5757 [15] is usually used to determine the air jet index (AJI) of materials, which represents the attrition loss of materials after certain period. Using this standard, Cabello et al. [5] evaluated the attrition of 23 different oxygen carriers with four different basis metals for the purposes of screening for use in CLC. However, this method often requires a substantial amount of particles and hours of analysis time. To tackle this issue, Rydén et al. [16] constructed a customized jet cup device, which is able to examine only a few grams oxygen carriers for chemical looping combustion (CLC), and successfully evaluated 25 different oxygen carrier materials comprehensively. In a similar manner, Amblard et al. [17] investigated the attrition caused by mechanical stress on both Group A FCC catalyst and Group B CLC oxygen carrier particles and compared the results with CFD modelling. With respect to non-oxygen carrier particles, Knight et al. [18] examined the attrition of CO_2 sorbent particles while Kim [19] investigated both CLC oxygen carriers and CO_2 sorbent particles.

The crushing strength [20,21] of oxygen carrier materials have also been evaluated many times. Crushing strength has been expected as an indicator of oxygen carrier's performance in a fluidized bed [14]. Crushing strength of a number of particles can be measured according to the standard method ASTM D-4179 [4,22] or by simply using a dynamometer [23,24]. In practice, the crushing strength value of a particle should be considered complimentary to the attrition rate in providing important estimations on the performance of oxygen carriers in a continuous operation [14].

Due to various available techniques in estimating attrition rate as well as crushing strength, there is currently not a universally applicable way to perform and interpret the mechanical strength of oxygen carriers. Still, any chosen method can be useful for screening and comparing various oxygen carrier materials as long as the aims and conditions are justified. For instance, utilizing the standard AJI measurement method is not applicable in this study as the amount of samples obtained are not sufficient, so evaluations in the customized jet cup rig is preferred. Even though it is then not possible to establish a standardized attrition resistance, it is known that materials that perform well in a large-scale unit at elevated temperatures often perform well in the attrition evaluation in a customized jet cup device, too [16]. Thus, the results are still useful as an indicator to what can be expected from the material if used as oxygen carriers in a large-scale fluidized bed unit, including chemical looping processes.

The novelty of this study lies in the aim to take the oxidation degree of oxygen carriers into account. With the change in oxidation degree, the chemical phases in the oxygen carriers will also change. We hypothesized that such a phase transformation may influence attrition resistance of the oxygen carriers, either directly or indirectly. An example of a direct effect could be if certain chemical phases are proved to be significantly more resistant to attrition. However, such a phenomenon is difficult to assess in the case of iron oxide phases. For instance, while the phase of metallic iron is logically harder than any iron oxide phases, there is no strong evidence that this is directly applicable to the attrition resistance of a material. Furthermore, none of the investigated materials in this study comprises 100% iron, which implies that the other elements can also affect the attrition rate of the material. Therefore, an indirect effect is more likely, that is, the chemical phase change may change the structure of the materials, which eventually leads to a change in its attrition rate [14]. This may include changes in porosity as well as elemental distribution.

In this study, we investigated the attrition rate of five iron-based oxygen carriers at different oxidation degrees in the customized jet cup device built and used by Rydén et al. [16]. To tackle the issue that the device cannot incorporate the effect of chemical stresses, the oxidation levels of the materials were set in a batch fluidized bed reactor through multiple redox cycles. The aim was to obtain materials with a similar chemical phase and mechanical structure to what would be expected should they were utilized in a chemical looping setup at elevated temperatures. Thus, the oxygen carriers were first exposed to certain chemical stresses in the batch fluidized bed reactor before they encountered mechanical stress in the jet cup rig. Furthermore, a crushing strength test was also performed to complement the attrition evaluation. By doing these experiments, we expected to be able to determine the correlation between attrition resistance (as well as crushing strength) and phase composition. XRD and SEM/EDX were used to characterize the crystalline phases and elemental composition of the materials, respectively.

2. Material and methodology

2.1. Oxygen carriers

Five different oxygen carriers were examined in this study: ilmenite ore, synthetic ilmenite, iron sand, LD slag, and mill scale. Additionally, quartz sand (assumed as pure SiO_2) was also examined as a reference material. A detailed general information about the oxygen carrier materials, including composition, is presented in Table 1 from a previous reference [25].

All the oxygen carriers were calcined in a high-temperature oven at 950 °C for at least 12 h in air and then sieved to 125–180 μm size range. Twenty grams of each material were then exposed to ten redox cycles in a fluidized bed batch reactor at 900 °C and subsequently prepared at three different mass conversion degrees (ω) after the 11th cycle. Within every of the first ten cycles, oxygen carrier was always completely oxidized before it was reduced with syngas (450 ml/min) for 20 s. An inert phase was introduced between each mentioned step to purge the remaining gas from the previous step. These ten cycles can be regarded as a way of stabilizing reactivity and, more crucially, obtaining a material with a mechanical and chemical structure which would be similar to what could be expected in a real chemical looping unit. This is because fresh oxygen carriers usually have less surface area and are less porous than the activated ones. Furthermore, exposure to redox cycles helps distribute oxygen throughout the whole particle, so this step is necessary to optimize the oxygen carrier performance. Here, the eleventh cycle was chosen as the cycle where the oxygen carrier was reduced

Table 1
Information about oxygen carrier materials.

Oxygen carrier	Elemental composition in atomic % (Oxygen-free basis)					General information
	Fe	Mn	Ti	Si	Ca	
Ilmenite ore	50	0.72	48	0.44	0.12	Mined by Titania A/S in Norway
Synthetic ilmenite	50	–	50	–	–	Synthesized by CSIC in Spain
Iron sand	50	0.50	0.22	45	4.54	By-product from the copper plant Boliden AB in Sweden
LD slag	22	3.46	1.2	15	58	By-product from the steel producer LKAB in Sweden
Mill scale	91	0.88	–	7.6	–	Steel rolled sheet residue from LKAB in Sweden

for a certain period which leads to its final mass conversion degree. So, all materials had been exposed to the same conditions except for the 11th cycle. The oxygen carriers are expected to have an already stable reactivity as well as mechanical structure after ten redox cycles. To ensure that the materials remain in the final mass conversion degree, an inert atmosphere (100 vol% N_2) was immediately fed into the reactor upon the completion of the reduction step and the furnace was switched off to allow a quick cooling down. It usually takes around 2 h to cool down the reactor from 900 °C to room temperature (25 °C). Here, mass conversion degree indicates the oxidation degree of an oxygen carrier, with $\omega = 1$ indicates a fully oxidized state. At last, each material was made available in four different oxidation states, which comprise the fresh-calcined state (without exposure in fluidized bed) and three different oxidation degrees, i.e., mass conversion degrees, which were prepared in a batch fluidized bed.

Table 2 shows the summarized procedure for a single redox cycle in the fluidized bed setup. The details of the fluidized bed setup can be found elsewhere [26]. The online measurement of outlet gas concentrations was done using a Rosemount™ NGA 2000 NDIR gas analyzer, which has up to ±1% repeatability at a constant temperature. Depending on the gas, the fluidization velocity ranged from 0.02 to 0.04 m/s, which corresponds to approximately 1.6–3.7 times the minimum fluidization velocity, respectively.

2.2. Attrition resistance investigation

The attrition resistance of each oxygen carrier sample prepared in the fluidized bed was tested in a customized jet cup rig device, which is illustrated in Fig. 2. There are several reasons behind using this device to correlate the oxidation degree with the attrition tendency of the oxygen carrier materials.

i) Performing a direct physical modelling of oxygen carrier attrition in a real continuous fluidized bed system entails a challenge to establish a comparable basis for evaluation. For instance, in a circulating setup, the oxygen carrier bed may likely be a mixture of particles with different mass conversion degrees. This implies that it is not possible to ensure a uniform oxidation degree of the oxygen carrier sampled from a circulating unit. Therefore, the most applicable evaluation strategy remains a correlative study [17].

ii) The use of a jet cup device is one of the most known methods to evaluate attrition tendency in correlation with fluidized bed conditions. Since in our case we do not use the standard ASTM method due to the small amount of sample, we may not be able to estimate the actual attrition rate in a real chemical looping unit. Still, the results are applicable enough for the sake of comparing the attrition tendency of various oxygen carriers and correlate it with the oxidation degree set in a fluidized bed setup, which is the aim of this study. The rig design itself allows the gas inlet to flow in a tangential flow, mimicking particle-wall collisions (mechanical stress) in cyclones, fluidized bed, and risers [27].

Five grams of each sample was put into the metal cup holder at the bottom of the rig. A flow of ten liters per minute of air (25 °C, 1 atm) was first flown into a humidifier containing a 25-cm water column. This was done to minimize the risk for static electricity in the settling chamber, which lead to particles sticking to the chamber wall. The humidified air flow was then fed into the jet cup rig from the inlet nozzle (inner diameter = 1.5 mm) placed tangentially at the bottom of the cup holder. This air flow creates an upward particle vortex throughout the cup and eventually into the settling chamber. The oxygen carrier particles will experience mechanical stress during this process due to the high air velocity and harsh physical environment inside the apparatus. Eventually, heavier particles with generally larger size will fall back into the cup, while the generated fines will be carried toward the outlet and trapped by the 0.01 μm-filter. The filter is weighed every 10 min for an hour in order to estimate the attrition resistance of the particles. At the end of the experiment, both samples left in the cup holder and trapped in the filter were collected for further analysis. More details of this apparatus have been reported elsewhere [16].

Table 2
Procedure for a single redox cycle in the fluidized bed batch reactor.

Step	Gas	Volumetric flow at 25 °C and 1 atm (ml/min)	Duration (s)	Note
Oxidation	5% O_2 in N_2	1000	Until the OC becomes fully oxidized	Until the outlet O_2 concentration returns to 5%
Inert	100% N_2	1000	180	To purge the remaining gas out from the reactor
Reduction	50% CO in H_2 (syngas)	450	20	This value is only valid for the mentioned ten redox cycles. For the 11th cycle, this value varies between different oxygen carrier – fuel pairs.
Inert	100% N_2	1000	180	To purge the remaining gas out from the reactor

2.3. Crushing strength investigation

The crushing strength of a single oxygen carrier particle was measured by using a Shimpo FGE digital force gauge FGN-5B with a maximum load of 50 N and an accuracy of 0.01 N. One hundred randomly selected particles from each sample bulk were crushed and the corresponding crushing force was measured using the device [5].

2.4. Characterization

The crystalline phases of each examined material were investigated using XRD D8 Discover. The sample topography of the bulk samples was examined using Phenom ProX SEM/EDX. The elemental composition of the bulk samples, i.e., before jet cup examination, and collected fines from the filter were characterized under SEM/EDX using FEI ESEM Quanta 20, which comes with a higher resolution imaging as this is deemed suitable for small fines. For the bulk samples, a semi-quantitative analysis was performed based on the XRD results in order to compare the phases on the surface of the oxygen carriers to those observed in the collected fines. This was done by converting the peak ratios of the detected phases to mass ratios [28].

2.5. Data analysis

The oxidation degree of an oxygen carrier is presented as mass conversion degree. Syngas conversion gives the following mass conversion degree formula,

$$\omega = 1 - \int_{t_0}^{t} \frac{\dot{n}\, M_O}{m_{ox}} \left(2x_{CO_2} + x_{CO} - x_{H_2}\right) dt \quad (1)$$

with

M_O = molecular weight of oxygen.
m_{ox} = mass of oxygen carrier at its fully oxidized state.
$\dot{n}$= outlet molar flow.
t = reaction time.
x_i = molar fraction of species *i*.
ω_i = mass conversion degree of the oxygen carrier upon conversion of species *i*.

The attrition resistance of each sample can be quantified in attrition

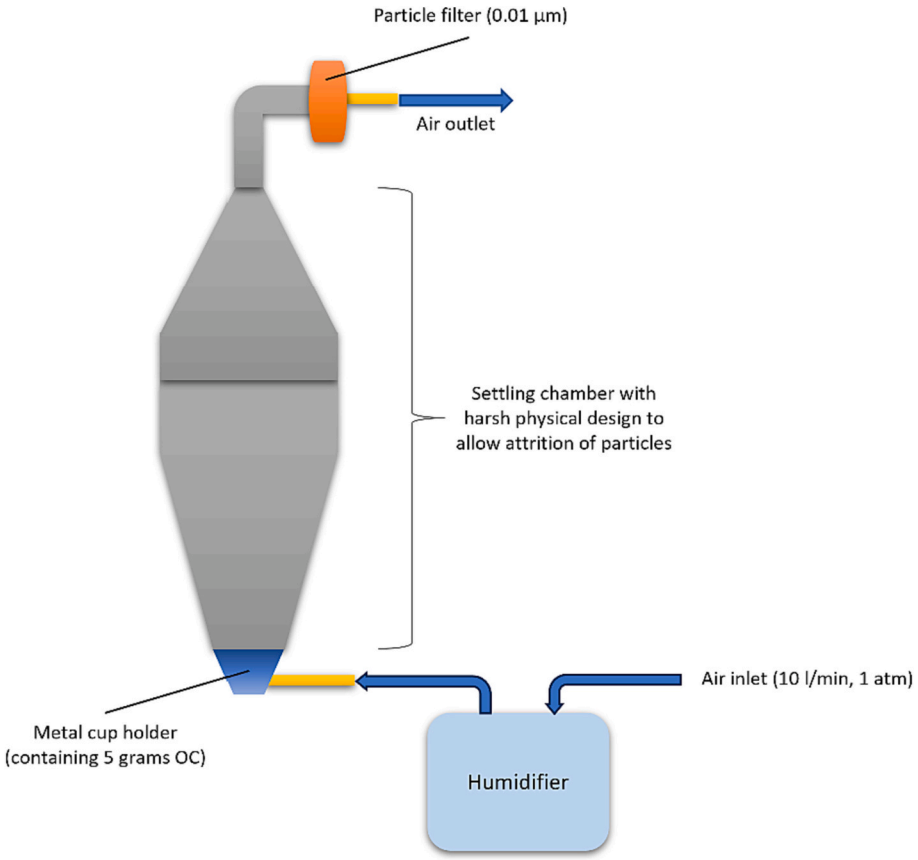

Fig. 2. Schematic diagram of the customized jet cup rig device.

rate A (in wt%/h), which is defined as the amount of generated fines divided by mass of the initial bulk sample (about 5 g) collected over a certain time, i.e., 10 min for each increment (see sub-section 2.2).

$$A = \frac{mass\ of\ collected\ fines\ (g)}{initial\ mass\ of\ bulk\ sample\ (g) \times observation\ time\ (h)} \times 100\% \quad (2)$$

The crushing strength is the average value from the measurement of 100 randomly selected oxygen carrier particles.

3. Results

3.1. Mass conversion degree and crystalline phases

Mass conversion degree (ω) indicates the oxidation levels of an oxygen carrier. A fully oxidized oxygen carrier is always assigned with a mass conversion degree of 1, suggesting a maximum oxidation level an oxygen carrier may have. Fig. 3 illustrates the theoretical correlation between phase transformation and mass conversion degree for an Fe-material. Suppose an oxygen carrier is entirely composed of pure iron oxides, its fully oxidized form will comprise 100 wt% Fe_2O_3. As the material gets reduced, parts of Fe_2O_3 will gradually transform to Fe_3O_4, which can be assumed as a combination of Fe_2O_3 and FeO. At a theoretical mass conversion degree of around 0.9, the oxygen carrier will comprise 100 wt% FeO. If the reduction continues, the whole oxygen carrier will eventually lose all its available oxygen, leaving only metallic iron within at a theoretical mass conversion degree of around 0.7. Note that mass conversion degree can never be zero, the remaining metallic iron still has a measurable mass. In this study, none of the materials is composed of pure iron oxides, so the value of mass conversion degree may be different (usually higher due to the lower iron content) from that illustrated here for similar chemical phases. In addition to the iron oxide phases, other combined oxides may also form due to the interactions

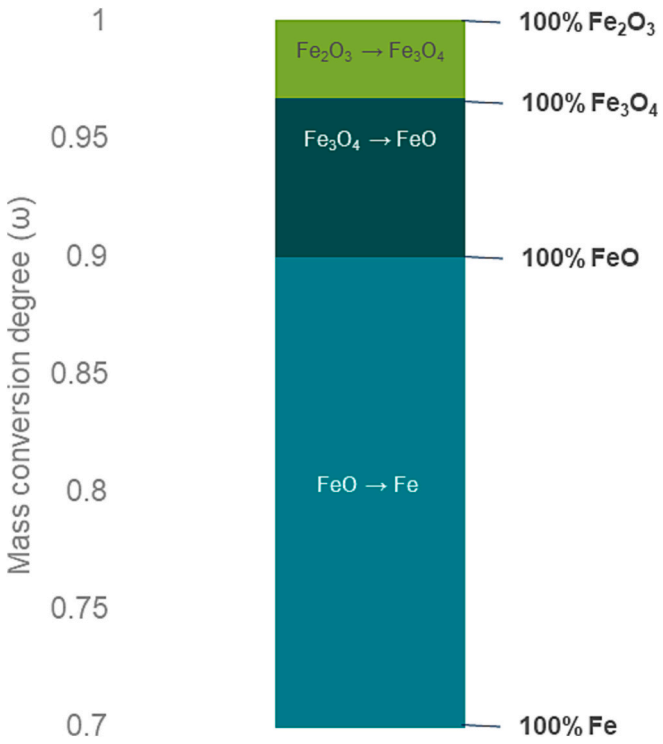

Fig. 3. Theoretical correlation between phase transformation and mass conversion degree.

between Fe and other constituents, e.g., Si, Ca, etc., see the phase analysis in Table 4.

The mass conversion degree (ω) of the oxygen carrier samples was set in a fluidized bed setup. Calculated based on Eq. 1, the mass conversion degree values are presented in Table 3. Both the freshly calcined and fully oxidized samples have a mass conversion degree of 1 – the only difference is that the former was prepared in a high-temperature oven, while the latter was cycled in the fluidized bed setup for 11 cycles. The uncertainty of the mass conversion degree is largely affected by the gas analyzer, which has a repeatability of ±1% in measuring outlet gas concentrations (in volume percentage). Since the mass conversion degree in this work is presented in fractions, this entails a standard deviation of ±0.0001.

Among all the investigated samples, mill scale was able to undergo the furthest reduction without experiencing defluidization. Mill scale contains almost 100% iron oxide [29], which likely means a much higher oxygen transfer capacity, thereby allowing further reduction. The other materials have been known for their defluidization tendency when exposed to a high reduction degree [30], thus the reduction extent is limited in this study to avoid defluidization in the fluidized bed.

As explained above, mass conversion degree change means changes in oxygen carrier's crystalline structure. We expected that phase composition contributes to the structure of the particles and may, therefore, have an implication on the mechanical strength. The crystalline phases on the oxygen carriers, which were obtained from the XRD analysis using a molybdenum source, are presented in Table 4. The phase name can be found after the table.

3.2. Attrition resistance

During the investigations using the customized jet cup device, each material showed a different attrition rate tendency. Rydén et al. [16] has previously reported that the attrition tendency of an oxygen carrier may follow either a linear or a non-linear trend as a function of time. Fig. 4 below illustrates both attrition rate tendencies (see Eq. 2 for calculation) observed during our study in the case of ilmenite ore. There, A_{tot} and $A_{30–60}$ refer to the total attrition rate observed during the whole 60-min investigation and the attrition rate in the last 30 min in the observation, respectively. It can be seen that the freshly calcined ilmenite ore tends to experience a linear total attrition [31], while the fully oxidized one follows a non-linear one.

In this work, we observed that the total attrition rate of most oxygen carrier samples follows a non-linear trend. Still, the attrition rate in the last 30 min of all samples during the observations tends to show a rather linear trend [16] (see the solid lines in Fig. 4). Therefore, this attrition rate, symbolized as $A_{30–60}$, is taken as the basis of comparison. Fig. 5 shows the attrition rate $A_{30–60}$, presented in bar columns, measured for different oxygen carrier materials at different mass conversion degrees, refer to left y-axis. Additionally, the attrition rate ratio between $A_{30–60}$ and A_{tot} is also presented as line in the same graph, refer to the right y-axis. An attrition rate of 1 indicates a perfectly linear attrition [16]. Sand is shown as a reference.

The attrition rate tendency changes between different materials. Sand as the reference material, which is a common bed material in circulating fluidized bed units, has an attrition rate and an attrition rate ratio of around 0.5 wt%/h and 0.75, respectively. Both ilmenite ore and iron sand have shown a relatively stable attrition rate over different mass conversion degrees, even though the former show a slight attrition

Table 3
Mass conversion degree of the oxygen carrier samples.

Oxygen carriers	Fully oxidized (FO)	Moderately reduced (MR)	Substantially reduced (SR)
Ilmenite ore	1.000	0.991	0.980
Synthetic ilmenite	1.000	0.990	0.979
Iron sand	1.000	0.992	0.983
LD slag	1.000	0.993	0.988
Mill scale	1.000	0.958	0.914

Table 4
Crystalline phases on oxygen carriers' surface observed by XRD.*

Oxygen carrier	Mass conversion degree	Crystalline phases
Ilmenite ore	1.000 (freshly calcined)	Fe_2TiO_5, Fe_2O_3, TiO_2
	1.000 (fully oxidized)	Fe_2TiO_5, Fe_2O_3, TiO_2
	0.991	Fe_2TiO_5, $FeTiO_3$, TiO_2
	0.980	Fe_2TiO_5, Fe_2O_3, Fe_3O_4, TiO_2
Synthetic ilmenite	1.000 (freshly calcined)	Fe_2TiO_5, Fe_2O_3, TiO_2
	1.000 (fully oxidized)	Fe_2TiO_5, Fe_2O_3, TiO_2
	0.990	Fe_2TiO_5, $FeTiO_3$, TiO_2
	0.979	Fe_2TiO_5, $FeTiO_3$, TiO_2
Iron sand	1.000 (freshly calcined)	Fe_2O_3, Fe_3O_4, SiO_2
	1.000 (fully oxidized)	Fe_2O_3, Fe_3O_4, SiO_2
	0.992	Fe_2O_3, Fe_3O_4, Fe_2SiO_4, SiO_2
	0.983	Fe_2O_3, Fe_3O_4, FeO, SiO_2
LD slag	1.000 (freshly calcined)	Fe_2O_3, Fe_3O_4, $Ca_2Fe_2O_5$, Ca_2SiO_4, CaO
	1.000 (fully oxidized)	Fe_2O_3, Fe_3O_4, $Ca_2Fe_2O_5$, Ca_2SiO_4, CaO
	0.993	Fe_3O_4, $Fe_{11}O_{12}$, $Ca_2Fe_2O_5$, Ca_2SiO_4, CaO
	0.988	Fe_3O_4, $Fe_{1-\delta}O_{12}$, $Ca_2Fe_2O_5$, Ca_2SiO_4, CaO
Mill scale	1.000 (freshly calcined)	Fe_2O_3
	1.000 (fully oxidized)	Fe_2O_3
	0.958	Fe_3O_4, FeO
	0.914	Fe_3O_4, FeO, $Fe_{1-\delta}O$, Fe

* Phase name: Fe_2O_3 = hematite, Fe_3O_4 = magnetite, $FeO/Fe_{1-\delta}O/Fe_{11}O_{12}$ = wüstite, Fe = metallic iron, $FeTiO_3$ = ilmenite, TiO_2 = rutile, SiO_2 = cristobalite, $Ca_2Fe_2O_5$ = srebrodolskite, Ca_2SiO_4 = larnite, CaO = lime

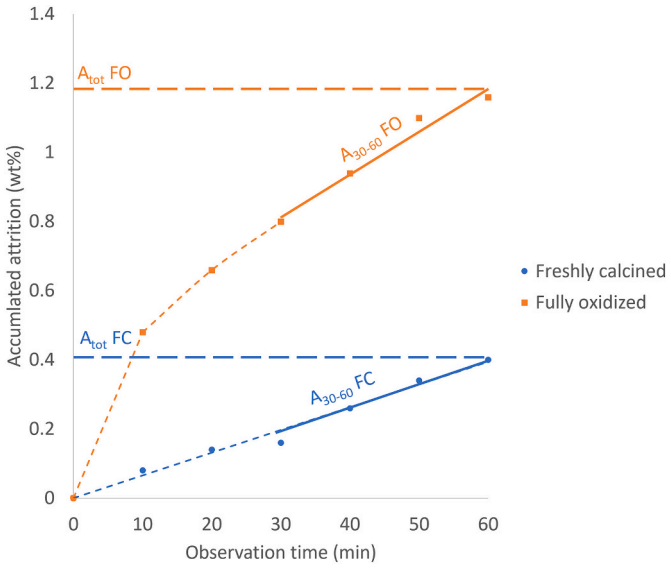

Fig. 4. Different attrition rate tendencies observed on the freshly calcined (FC) and fully oxidized (FO) ilmenite ore, which shows linear and non-linear total attrition trends, respectively. The solid and dashed lines refer to the attrition rate $A_{30–60}$ and A_{tot}, respectively.

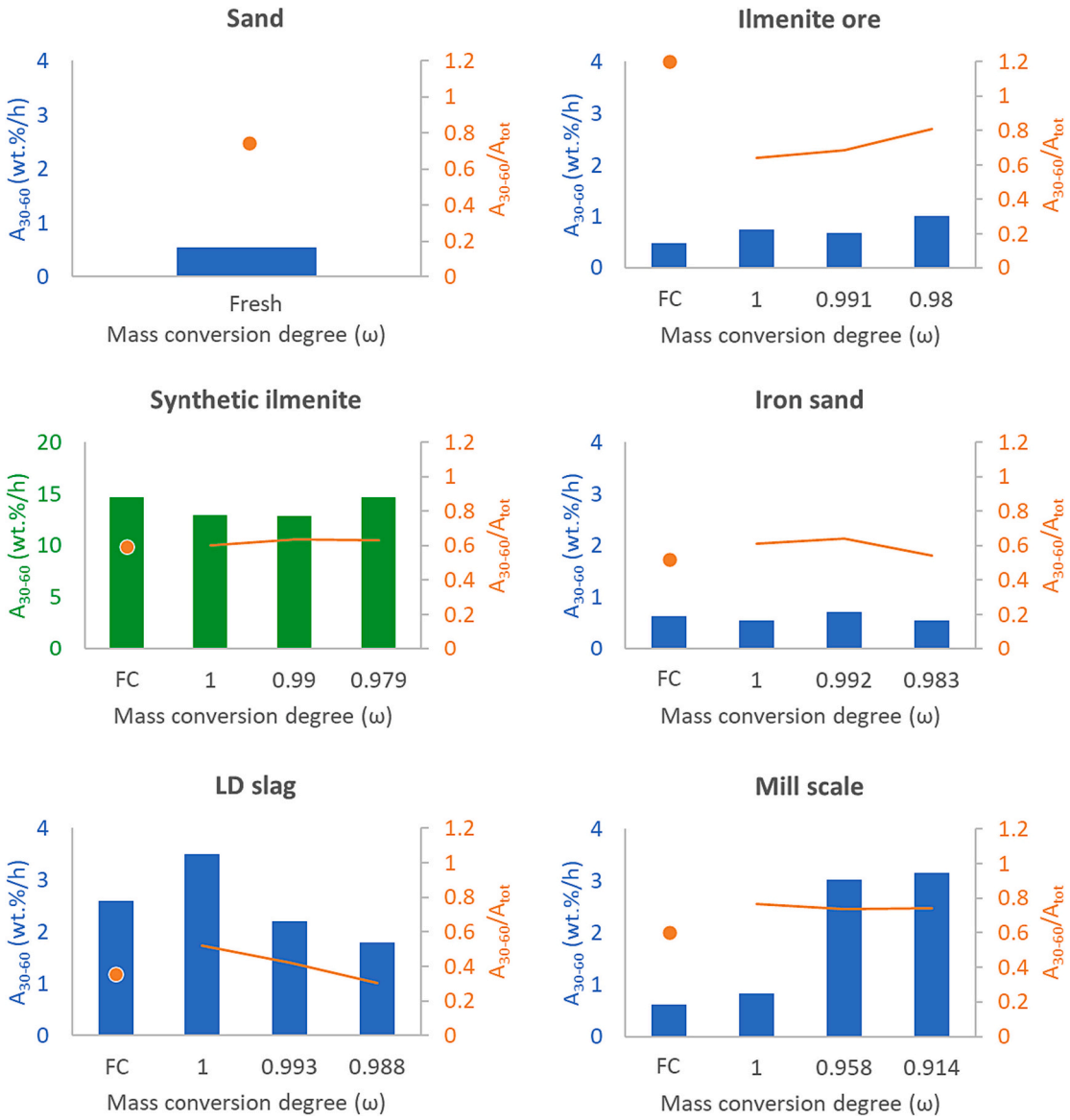

Fig. 5. The attrition rate A_{30-60} (presented in bar columns) and the attrition rate ratio A_{30-60}/A_{tot} (presented as lines) for different oxygen carriers at different mass conversion degrees. FC denotes the freshly calcined state of each material. Note that the synthetic ilmenite has a different Y-axis scale for A_{30-60}.

rate increase. Furthermore, both the mentioned materials also show the lowest attrition rates of all investigated materials. Iron sand performed slightly better with attrition rates which are similar to that of sand, i.e., about 0.5–0.7 wt%/h, while those of the ilmenite ore are between 0.6 and 1 wt%/hour.

LD slag and mill scale show opposing attrition rate tendencies. While the attrition rate of LD slag tends to decrease at lower mass conversion degree, that of mill scale increased substantially. However, it is important to note that mill scale has been reduced substantially further than the other materials – this was possible due to its higher Fe content. Both the freshly calcined and fully oxidized mill scale have similar attrition rates with those of the ilmenite ore, which has been found among the strongest materials in this study.

Being the only synthetized material in this study, the synthetic ilmenite has the lowest attrition resistance among all investigated materials. Please note the different scaling on the axes for this material in Fig. 3. The attrition rate of the substantially reduced synthetic ilmenite is higher than that at higher mass conversion degrees but similar to that of the freshly calcined one.

Most activated samples, i.e., non-fresh materials, have a lower attrition rate ratio than that of sand, which indicates that the attrition rate of the investigated oxygen carriers saw a more substantial decrease compared to sand after 30 min. The majority of oxygen carrier samples, except LD slag, has a rather stable attrition rate ratio independent of mass conversion degree. LD slag shows a declining attrition rate ratio.

3.3. Chemical analysis of the generated fines

Fines collected from the customized jet cup device were characterized using SEM/EDX using a point analysis. The sampling was performed by considering different contrasting particles observed under SEM/EDX and at least 5 points were observed for each bulk sample over multiple particles. The estimated elemental composition of the fines for the fully oxidized (FO) samples and substantially reduced (SR) samples were calculated as the average composition from the observable points and are shown in Table 5. FC (ref) is the composition of the freshly calcined material according to the available data (see Table 1) [25]. Note that the freshly calcined (FC), instead of fully oxidized (FO), mill scale was presented here due to the lack of possibility to recover the FO fines. Still, this is expected to be sufficiently representative as their bulk

Table 5
Average elemental composition on the surface of the collected fines from each oxygen carrier at their fully oxidized (freshly calcined for mill scale) and substantially reduced forms observed under SEM/EDX using point analysis.

Oxygen carrier	Sample	Elemental composition, in atomic %				
		Fe	Mn	Ti	Si	Ca
Ilmenite ore	FC (ref)	50	0.72	48	0.44	0.12
	FO	70	0.73	17	8.7	3.7
	SR	60	0.77	32	5.3	1.2
Synthetic ilmenite	FC (ref)	50	0	50	0	0
	FO	56	0	42	1.1	0.1
	SR	55	0	43	1.3	0
Iron sand	FC (ref)	50	0.50	0.22	45	4.54
	FO	71	1.1	1.3	17	10
	SR	74	1.0	0.54	16	7.9
LD slag	FC (ref)	22	3.46	1.2	15	58
	FO	19	3.7	1.7	9.5	66
	SR	24	3.9	1.3	9.6	62
Mill scale	FC (ref)	91	0.88	0	7.6	0
	FC	92	0.75	0.19	1.8	4.3
	SR	97	0.66	0	0.49	1.5

crystalline chemical phases are nearly identical (see Table 4).

It is clear from the point analysis that the fines from the ilmenite ore, mill scale and iron sand have a considerable enrichment of iron compared to the original samples. This is not the case with that obtained from the synthetic ilmenite, which has a ratio of about 50/50 between Fe and Ti, which also is the atomic ratio of the original sample, see Table 1. The fines coming from LD slag are clearly rich in calcium. Note that Mn, Si, and Ca contents in fully oxidized and substantially reduced iron sand and Ti and Mn contents in fully oxidized and substantially reduced mill scale are most likely impurities obtained from the jet cup device filter, which have been used for the examination of the other samples.

The result of the SEM/EDX analysis can be further compared to the XRD results (see Table 4) of the fully oxidized and substantially reduced bulk samples, i.e., before jet cup examination, using a semi-quantitative analysis. As we did not crush the samples, we expected to get representative results from the oxygen carriers' surface rather than from inside the bulk. The summary is shown in Fig. 6 below.

Fig. 6 illustrates the phase transformation on the oxygen carriers' surface obtained from a semi-quantitative analysis. Even though such an analysis can entail quite large errors; some general conclusions can still be made. Substantially reduced ilmenite ore clearly has much higher hematite and significantly less pseudobrookite compared to its fully oxidized counterpart. A similar pattern can be seen with synthetic ilmenite. The substantially reduced iron sand has much more magnetite than the fully oxidized one as well as a minor amount of wüstite. LD slag does not experience significant transformation, except in the cases of hematite reduction to magnetite and even wüstite. Nearly all hematite in the fully oxidized mill scale has been reduced to magnetite, largely wüstite, and a minor amount of metallic iron in the substantially reduced one.

3.4. Crushing strength

The average crushing strength from 100 examined particles is presented in Fig. 7. The mass conversion degrees of all materials, expect mill scale, are quite similar to two-digit accuracy, therefore they are shown together in a single column bar graph. Mill scale is thus shown in another graph due to the large differences in its mass conversion degrees. The error bars show the upper and lower 95% confidence intervals.

Among the investigated oxygen carriers, iron sand has the highest crushing strength values, especially on its freshly calcined state (about 5 N). This is in line with our observation that the calcined iron sand taken from the high-temperature oven was the most difficult material to break into smaller pieces. Iron sand at $\omega = 0.99$ seems to have a slightly higher crushing strength than the fully oxidized one ($\omega = 1$), but the same sample also has the highest standard deviation, which is presented as an error bar. Both these samples have a similar crushing strength of around 4–4.5 N. Iron sand at the lowest mass conversion degree clearly has the lowest crushing strength at about 2.5 N.

Comparing mill scale and the ilmenite ore, their fully oxidized samples have similar crushing strength values at about 3 N. However, ilmenite shows a significantly more stable crushing strength compared to mill scale independent of mass conversion degree. Still, it should be

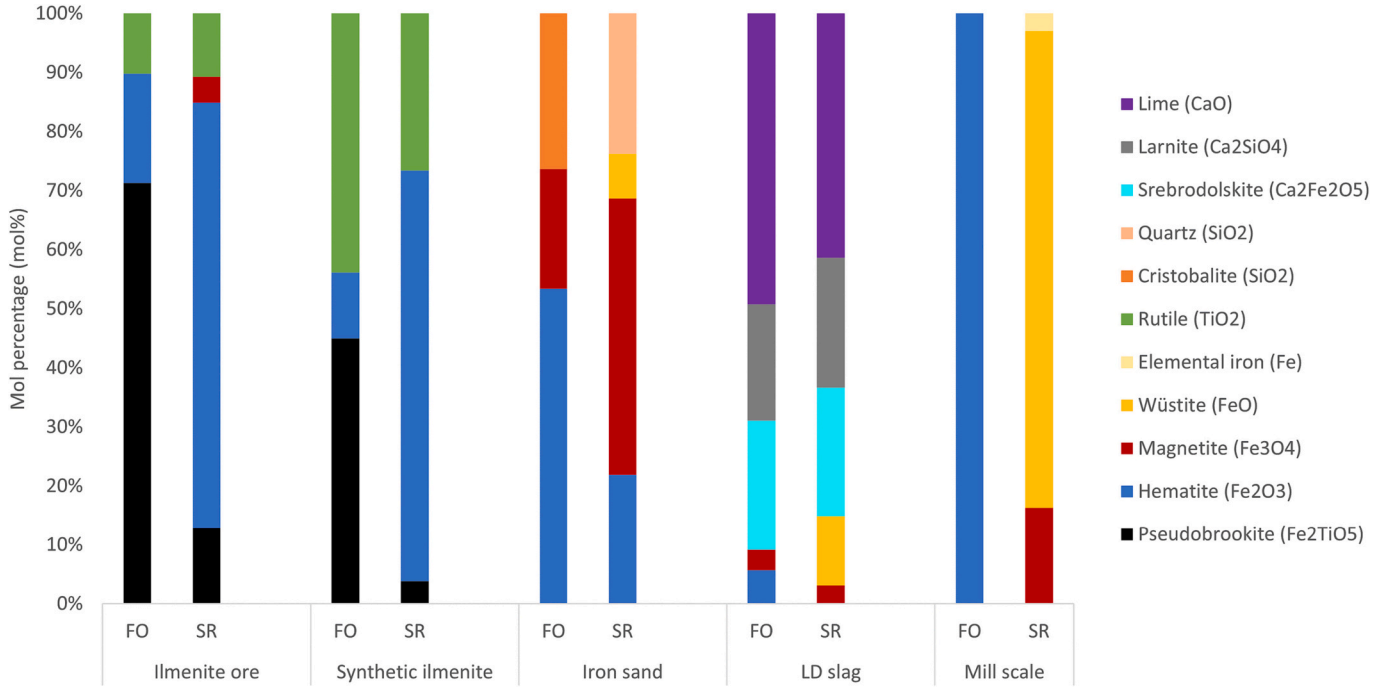

Fig. 6. Semi-quantitative analysis of the surface of fully oxidized (FO) and substantially reduced (SR) bulk oxygen carriers, i.e., before jet cup examination, based on the XRD results.

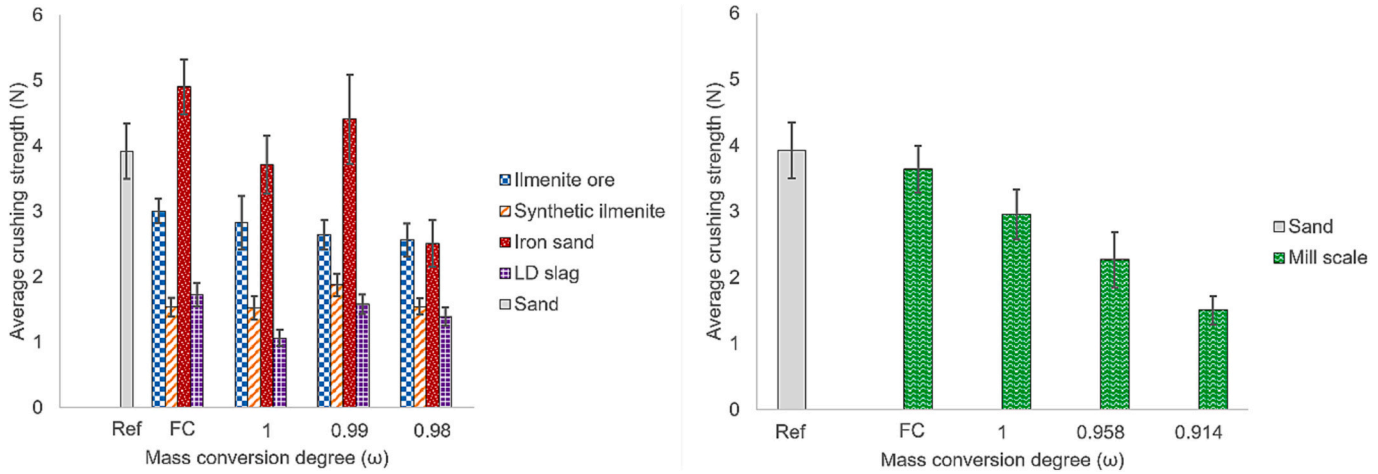

Fig. 7. The average crushing strength of a hundred particles randomly selected from each sample. Sand is shown as reference. Ref and FC denote the reference and a freshly calcined state, respectively.

noted that mill scale got reduced much further than ilmenite in this study. Even at its lowest mass conversion degree (ω = 0.914), its crushing strength is still on a par with that of other materials at their lowest ω such as LD slag and synthetic ilmenite – both did not get reduced as far as mill scale.

Lastly, both synthetic ilmenite and LD slag have a fairly similar and stable crushing strength, which are quite low at about 1.5 N in most cases. Similar to iron sand, both materials also have their lowest and highest crushing strength values at their fully oxidized states (ω = 1) and ω = 0.99, respectively. Still, their crushing strength values are generally lower than those of the other materials.

Fig. 8 is a plot between crushing strength and attrition rates of the activated samples, i.e., the samples that have been exposed to redox cycles in the batch fluidized bed reactor. This means all the freshly calcined samples are excluded from the plot. The reason for this is to have a better observation in order to see if the crushing strength and attrition rate correlate to each other. However, it is clear that the parameters do not show a strong correlation between each other as a higher crushing strength does not necessarily indicate a better attrition resistance and vice versa.

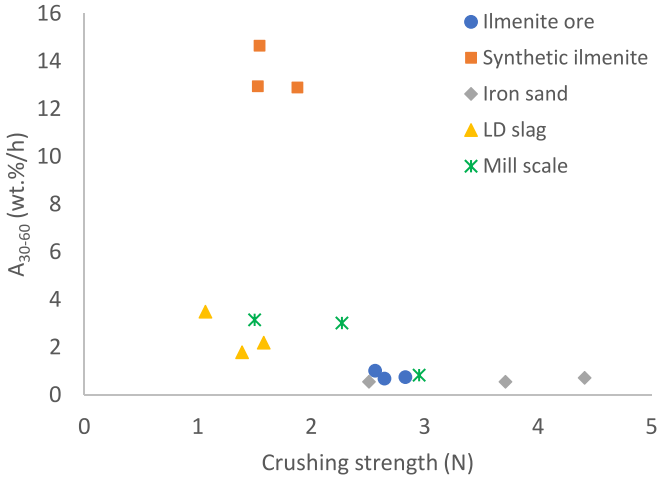

Fig. 8. Attrition rate plotted against crushing strength for all activated oxygen carriers.

4. Discussion

4.1. Oxygen carrier's mechanical strength over different mass conversion degrees

Ilmenite ore saw a slightly increasing attrition rate with an average value slightly higher than sand. Its crushing strength slightly decreases over different mass conversion degrees and is slightly lower than that of sand. These make ilmenite ore one of the most robust materials with quite a stable attrition rate and crushing strength in this study. The material has been reported to have a low attrition rate in a chemical looping combustion units [32]. Still, an increasing attrition rate was observed. An iron migration outward to the surface was observed, which leads to enrichment of iron on the surface (see Fig. 6) and a high iron content on fines (see Table 5).

On the other hand, synthetic ilmenite has shown the highest attrition rates among the evaluated oxygen carriers at all mass conversion degree. Its crushing strength values are also quite low despite undergoing a similar crystalline phase transformation with ilmenite ore. The major reason for this phenomenon is likely due to the synthesis process itself, which led to loosely sintered Fe_2O_3 and TiO_2 particles. This may have led to non-uniform grain sizes and, thus, a different diffusion process compared to that taking place in ilmenite ore [33]. Fig. 9 shows that the freshly calcined ilmenite ore shows a more uniform sintered surface compared to freshly calcined synthetic ilmenite under SEM observation. Additionally, the enrichment of iron also did not take place in the synthetic ilmenite like it did in ilmenite ore, see Table 5.

Contrary to the ilmenite ore, which had undergone harsher geological processes over millennia, synthetic ilmenite had never been exposed to such a treatment. This might be the reason why synthetic ilmenite behaves differently. Furthermore, Staničić et al. [34] has reported that synthetic ilmenite tends to be more porous than the ilmenite ore. A higher porosity has been reported to be one of the factors that cause a decreased attrition resistance [31,35]. Fig. 10 shows the SEM images of the collected fines from attrition examinations of fully oxidized ilmenite ore and synthetic ilmenite in the customized jet cup rig. The visualization clearly shows that the collected fines from ilmenite ore are significantly coarser and have sharper edges compared to that from synthetic ilmenite.

When it comes to waste materials, iron sand has quite a stable attrition resistance and its attrition rates are on par with those of sand, so this material is the most robust oxygen carrier in this study. The reported BET surface area of freshly calcined iron sand indicate a rather low porosity [36], which may contribute to its mechanical stability. We also observed that freshly calcined iron sand is quite difficult to break into

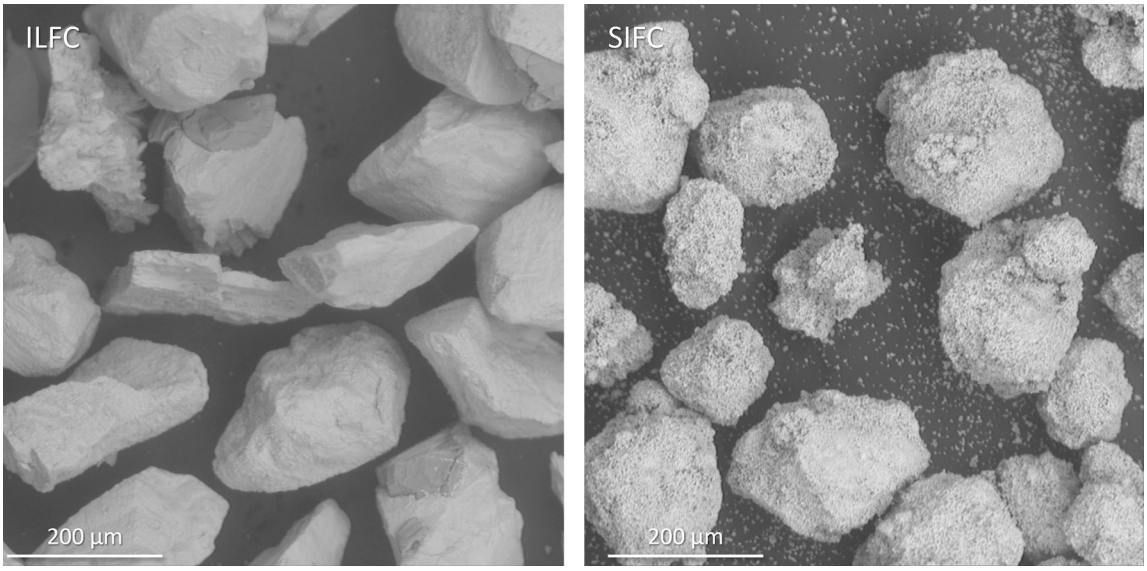

Fig. 9. SEM images of freshly calcined ilmenite ore (ILFC) and synthetic ilmenite (SIFC).

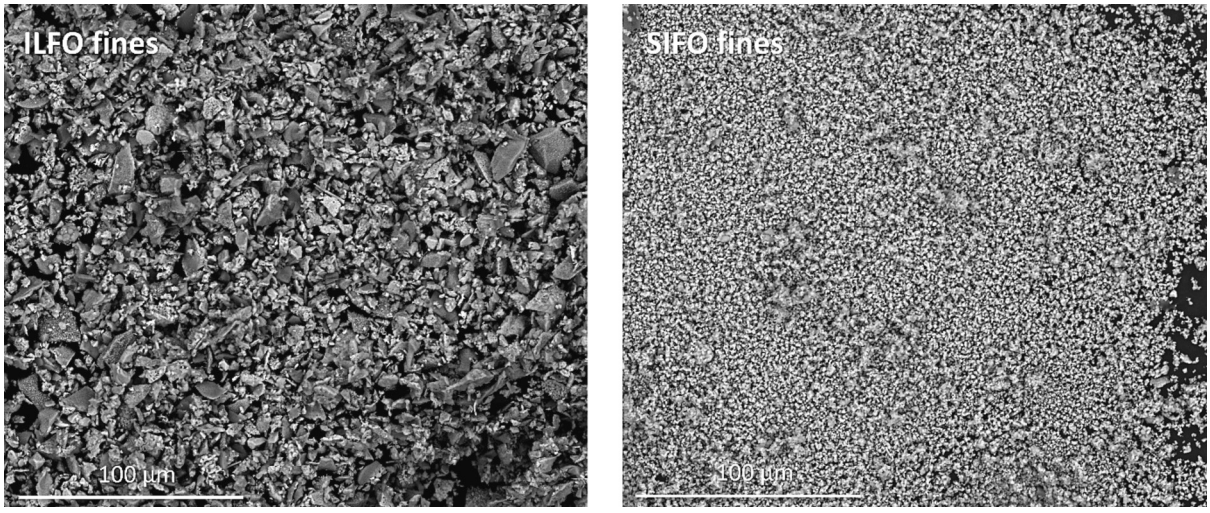

Fig. 10. SEM images of collected fines from attrition examinations of fully oxidized ilmenite ore (ILFO) and synthetic ilmenite (SIFO) in the customized jet cup rig.

smaller pieces, which indicates a strong sintering. The trend on iron sand's crushing strength is inconclusive, yet it is clear that the substantially reduced iron sand has the lowest crushing strength. This indicates that a stable attrition resistance does not necessarily lead to an uncompromised crushing strength, as the material may be robust toward mechanical erosion but not compressive load.

In general, LD slag shows higher attrition rates and lower crushing strength compared to sand. Some manganese ores with a significant CaO content have shown a similar attrition rate to LD slag in this study [37]. The fact that LD slag has multiple phases on its surface (see Fig. 6) may have led to a rather uneven phase distribution and, therefore, uneven strength throughout the particle. This likely causes a lower attrition resistance and crushing strength in general. LD slag has a relatively stable crushing strength, but this is not the case with its attrition rates, which decrease at lower mass conversion degrees. Hildor et al. [38] reported a decrease on the BET surface area of LD slag after activation, which suggests that the material becomes less porous during redox cycles. Furthermore, another calcium-based perovskite material has been reported to experience an improved attrition resistance after exposure to a continuous redox cycles [16], while LD slag contains a fair share of srebrodolskite (see Table 4 and Fig. 6), which also belongs to calcium-based perovskite phases. This likely has an implication to the increasing trend of its attrition resistance.

Mill scale has previously been reported to have a lower attrition resistance compared to the ilmenite ore [39], so it is reasonable that the material has significantly higher attrition rates than ilmenite ore and sand, especially at lower mass conversion degrees. The attrition resistance and crushing strength of mill scale tends to decrease as the material gets reduced further. Fig. 6 demonstrates that the freshly calcined mill scale is composed of almost entirely hematite, but its substantially reduced counterpart comprises largely magnetite and minor amounts of wüstite and elemental iron. The formation of these phases reportedly leads to more cracks and pores on the oxygen carrier's surface [40]. This may contribute to a decreasing mechanical strength of mill scale at lower mass conversion degrees.

As mentioned, our initial conjecture was that phase composition may affect the attrition rate trend. However, materials like ilmenite ore and iron sand show a stable attrition rate despite their phase composition changes, see Table 4. Still, in an attempt to build a generic hypothesis with respect to this, it can be useful to correlate the main metal bases of the materials to the attrition rate. Table 6 summarizes the main metal bases, the ratio of average attrition rates of the activated samples (taken

Table 6
Main metal bases, ratio of average attrition rate to that of sand, and attrition rate trend of examined oxygen carriers.

Oxygen carrier	Main metal bases	Ratio of average attrition rate to that of sand	Attrition rate trend over decreasing mass conversion degree
Ilmenite ore	Fe, Ti	1.4	Generally stable
Synthetic ilmenite	Fe, Ti	24.4	Generally stable
Iron sand	Fe, Si	1.1	Generally stable
LD slag	Fe, Ca	4.5	Decreasing
Mill scale	Fe	4.2	Increasing

from three different mass conversion degrees – the freshly calcined sample is excluded) to that of sand, and the attrition rate trend of the evaluated oxygen carriers.

From Table 6, it seems that both Fe-Ti and Fe-Si combinations contribute to a rather stable attrition rate over different mass conversion degrees. Furthermore, materials with these combinations show a comparable attrition rate to sand, except for synthetic ilmenite – this has been explained above. On the other hand, Fe alone tends to see a decrease in attrition resistance with further reduction, while a Fe-Ca system seems to contribute to an improved attrition resistance at lower mass conversion degrees. Our hypothesis is that this can be related to the psychochemical structure of the materials and how it changes with reduction [14]. This may include multiple factors such as porosity [3,41], sintering quality, and formation of iron layers [42] – all can play a role at the same time. However, assessing the influence of a single potential factor on the attrition rate of materials in general has been found challenging. For instance, a direct correlation between BET surface area and attrition rate has been deemed inconclusive [14]. Still, some publications hint on results that may support these findings. For instance, the addition of Fe reportedly increases the strength of Ti-based alloy materials at certain conditions [43,44] Also, Fe-Si alloys with >11 at.% Si have been found to show good mechanical properties [45]. An Fe-catalyst has been found to have a low attrition resistance [46]. However, we could not find any related references with respect to the Fe-Ca system by far.

Furthermore, the attrition resistance of an oxygen carrier seems to be a more significant parameter in comparing the mechanical strength of oxygen carriers, while the crushing strength is not so representative due to variations between different particles and, at times, inconclusive trends. This is despite the fact that we had measured the crushing strength of more particles than what have been previously done, i.e., 100 cf. as few as 20 particles in these publications [24,47]. Rydén et al. [16] have previously reported that a more suitable size range for a meaningful crushing strength investigation should be at least 180–250 μm cf. 125–180 μm in this case, yet this will still entail a substantial systematic measurement error. Some publications [48,49] that have successfully depicted relationships between particle size and crushing strength in a reliable way used particles with several millimeter sizes, so investigating small particles in the same manner has proven to be challenging as for now. Still, crushing strength measurement can still be useful for rejecting non-suitable materials as a low crushing strength almost always implies a poor fluidization performance [47]. As shown in Fig. 8, both attrition rate and crushing strength show a weak correlation to each other. Nevertheless, the same figure shows that the crushing strength of ilmenite ore and iron sand never got lower than 2 N, which is reportedly the threshold value for an oxygen carrier to be considered acceptable for continuous operations [16]. In this regard, despite the weak correlation, both the attrition rates and crushing strength examinations may qualitatively agree on which oxygen carrier should be recommended from mechanical strength perspective. It is expected, however, that compressive forces in a fluidized bed unit may cause less significant damage on the oxygen carrier compared to attrition-causing phenomena, e.g., mechanical abrasion and particle collision, in a chemical looping unit.

4.2. Implication for chemical looping application

The results may have three main implications for chemical looping technology:

i) Material screening with respect to mechanical strength and the influence of oxidation degree.

Choosing a suitable oxygen carrier is essential for any chemical looping process. By comparing the attrition tendency, this study can give a useful estimation for oxygen carrier screening with respect to mechanical endurance. As discussed, ilmenite ore and iron sand seem to be the most robust materials, LD slag and mill scale have a moderate mechanical strength, and synthetic ilmenite shows the poorest mechanical performance. Excluding the poorly performing synthetic ilmenite, it seems that Fe-Ti and Fe-Si systems contribute to a generally stable attrition rate over different oxidation degrees, which is desired. On the other hand, the Fe-Ca system in our study saw a decline in attrition rate at lower oxidation degrees, while an almost pure Fe system experienced an increasing attrition rate.

ii) Relevance to various chemical looping processes.

With respect to CLC and OCAC, the most relevant results may be the results involving higher mass conversion degrees (around $1 > \omega > 0.990$) since the reduction extent in these processes are expected to be low. In this case, ilmenite ore, iron sand, and mill scale seem to have the best attrition resistance levels, while LD slag shows a significantly higher attrition rate. However, the results at lower mass conversion degrees ($\omega < 0.990$) are relevant for processes like CLG, CLR, and CLWS where higher reduction degrees of oxygen carrier might take place. In such a situation, only ilmenite and iron sand can still be said to have the best attrition resistance, while mill scale likely shows a higher attrition rate compared to that of its fully oxidized form. Counter-intuitively, LD slag may in turn show an improved attrition resistance, as it experiences a reduced porosity which leads to a lower attrition rate at lower oxidation states. From this explanation, it is clear that different oxygen carriers may have different levels of attrition resistance depending on the chemical looping processes they are being utilized in.

iii) Lifetime estimation of oxygen carriers over different oxidation degrees based on attrition rates.

With respect to ilmenite ore and iron sand, which are the best performing materials in this study, the lifetime of the ilmenite ore and iron sand would be about 100–160 and 140–200 h, respectively, judging by their attrition rates taken from different oxidation states in this study. Note, however, that this might not reflect the reality in a chemical looping unit as the conditions inside those reactors are very different than that in the customized jet cup rig [16]. As a comparison, Linderholm et al. [50] has reported an estimated lifetime of 700–800 h for the same ilmenite ore in a 100 kW chemical looping setup, which is a circulated fluidized bed unit. This is reasonable since the conditions in the jet cup device might be much mechanically harsher than that in the chemical looping unit. Nevertheless, the roughly estimated lifetime values from this study still lies between the desired lifetime range in a chemical looping unit, which is reportedly 100–400 h [51]. This suggests that the utilization of the ilmenite ore and iron sand in any chemical looping unit may have an advantage due to their robust mechanical resistance.

5. Conclusions

Based on attrition resistance and crushing strength investigations, some conclusions can be taken:

- The effect of phase transformation on the attrition rate of oxygen carriers depends largely on the type of the material itself. It seems that Fe-Ti and Fe-Si systems contribute to a stable attrition rate

independent of mass conversion degree, while a Fe-Ca system may lead to a decreasing attrition rate at lower mass conversion degrees.
- Attrition rate is a better comparison for the mechanical strength of oxygen carriers compared to crushing strength, which entails a higher systematic error when examining small particles.
- Ilmenite ore and iron sand have a relatively stable attrition rate (only slightly affected by oxidation state) at about 0.5–1.0 wt%/h (comparable to sand) and most robust mechanical strength among the investigated materials.
- The attrition rates of LD slag and mill scale are generally lower than that of iron sand and ilmenite and clearly influenced by their oxidation degree. As the materials get reduced further, the attrition resistance of mill scale decreases but that of LD slag increases instead.
- The results of this study can be useful for material screening with respect to various chemical looping processes as well as to roughly estimate the lifetime of oxygen carriers.

CRediT authorship contribution statement

Victor Purnomo: Conceptualization, Data curation, Formal analysis, Methodology, Project administration, Software, Supervision, Validation, Visualization, Writing – original draft, Writing – review & editing. **Robin Faust:** Data curation, Formal analysis, Software, Validation, Visualization, Writing – review & editing. **Lidiya Abdisa Ejjeta:** Formal analysis, Investigation, Writing – review & editing. **Tobias Mattisson:** Conceptualization, Funding acquisition, Writing – review & editing. **Henrik Leion:** Conceptualization, Funding acquisition, Methodology, Resources, Supervision, Validation, Writing – review & editing.

Declaration of competing interest

The authors declare that they have no known competing financial interests or personal relationships that could have appeared to influence the work reported in this paper.

Data availability

Data will be made available on request.

Acknowledgments

This work is a part of the project EU CLARA (Chemical Looping Gasification for Sustainable Production of Biofuels) which has received funding from the European Union's Horizon 2020 research and innovation program under grant agreement No 817841. This study has also received fundings from the Swedish Energy Agency (Project 51430-1) and Stiftelsen ÅForsk (Project 20-269). Boliden AB is acknowledged for iron sand sourcing. The authors appreciate Erik Sandell and Mattias Hertzberg for performing parts of the experimental work in this study as a bachelor thesis project.

References

[1] Z. Yu, et al., Iron-based oxygen carriers in chemical looping conversions: a review, Carbon Resour. Convers. 2 (1) (2019) 23–34, https://doi.org/10.1016/j.crcon.2018.11.004.
[2] T. Roshan Kumar, T. Mattisson, M. Rydén, V. Stenberg, Process analysis of chemical looping gasification of biomass for Fischer-Tropsch crude production with net-negative CO2Emissions: part 1, Energy Fuel (2022), https://doi.org/10.1021/acs.energyfuels.2c00819.
[3] T.A. Brown, F. Scala, S.A. Scott, J.S. Dennis, P. Salatino, The attrition behaviour of oxygen-carriers under inert and reacting conditions, Chem. Eng. Sci. 71 (2012) 449–467, https://doi.org/10.1016/j.ces.2011.11.008.
[4] J. Adánez, L.F. De Diego, F. García-Labiano, P. Gayán, A. Abad, J.M. Palacios, Selection of oxygen carriers for chemical-looping combustion, Energy Fuel 18 (2) (2004) 371–377, https://doi.org/10.1021/ef0301452.
[5] A. Cabello, P. Gayán, F. García-Labiano, L.F. De Diego, A. Abad, J. Adánez, On the attrition evaluation of oxygen carriers in chemical looping combustion, Fuel Process. Technol. 148 (2016) 188–197, https://doi.org/10.1016/j.fuproc.2016.03.004.
[6] R.D. Tovar-Valencia, A. Galvis-Castro, R. Salgado, M. Prezzi, D. Fridman, Experimental measurement of particle crushing around model piles jacked in a calibration chamber, Acta Geotech. 18 (3) (2023) 1331–1351, https://doi.org/10.1007/s11440-022-01681-8.
[7] C. Liu, F. Liu, J. Song, F. Ma, D. Wang, G. Zhang, On the measurements of individual particle properties via compression and crushing, J. Rock Mech. Geotech. Eng. 13 (2) (2021) 377–389, https://doi.org/10.1016/j.jrmge.2020.06.009.
[8] L. Yang, et al., Collision characteristics and breakage evolution of particles in fluidizing processes, Fuel Process. Technol. 243 (October 2022) (2023) 107654, https://doi.org/10.1016/j.fuproc.2023.107654.
[9] W.G. Vaux, D.L. Keairns, Particle attrition in fluid-bed processes, in: J.R. Grace (Ed.), Fluidization, Plenum Press, New York, 1980, pp. 437–444 [Online]. Available: https://link.springer.com/chapter/10.1007/978-1-4684-1045-7_45?utm_source=getftr&utm_medium=getftr&utm_campaign=getftr_pilot.
[10] F. Scala, A. Cammarota, R. Chirone, P. Salatino, Comminution of limestone during batch fluidized-bed calcination and sulfation, AICHE J. 43 (2) (1997) 363–373, https://doi.org/10.1002/aic.690430210.
[11] F. Scala, R. Chirone, P. Salatino, Attrition phenomena relevant to fluidized bed combustion and gasification systems, in: Fluidized Bed Technologies for Near-Zero Emission Combustion and Gasification no. 1981, Woodhead Publishing, 2013, pp. 254–315, https://doi.org/10.1533/9780857098801.1.254.
[12] F. Miccio, A. Natali Murri, E. Landi, Synthesis and characterization of geopolymer oxygen carriers for chemical looping combustion, Appl. Energy 194 (2017) 136–147, https://doi.org/10.1016/j.apenergy.2017.03.005.
[13] A. Cuadrat, A. Abad, J. Adánez, L.F. De Diego, F. García-Labiano, P. Gayán, Behavior of ilmenite as oxygen carrier in chemical-looping combustion, Fuel Process. Technol. 94 (1) (2012) 101–112, https://doi.org/10.1016/j.fuproc.2011.10.020.
[14] F. Liu, et al., Attrition and attrition-resistance of oxygen carrier in chemical looping process – a comprehensive review, Fuel 333 (September 2022) (2023), https://doi.org/10.1016/j.fuel.2022.126304.
[15] ASTM, D5757–95 A. Standard Test Method for Determination of Attrition and Abrasion of Powdered Catalysts by Air Jets, 1995.
[16] M. Rydén, P. Moldenhauer, S. Lindqvist, T. Mattisson, A. Lyngfelt, Measuring attrition resistance of oxygen carrier particles for chemical looping combustion with a customized jet cup, Powder Technol. 256 (2014) 75–86, https://doi.org/10.1016/j.powtec.2014.01.085.
[17] B. Amblard, S. Bertholin, C. Bobin, T. Gauthier, Development of an attrition evaluation method using a Jet Cup rig, Powder Technol. 274 (2015) 455–465, https://doi.org/10.1016/j.powtec.2015.01.001.
[18] A. Knight, N. Ellis, J.R. Grace, C.J. Lim, CO2 sorbent attrition testing for fluidized bed systems, Powder Technol. 266 (2014) 412–423, https://doi.org/10.1016/j.powtec.2014.06.013.
[19] J.Y. Kim, Jet attrition characteristics of chemical looping oxygen carriers and CO_2 sorbents, University of British Columbia, 2020, https://doi.org/10.14288/1.0392791.
[20] E. Jerndal, et al., Utilisation de matériaux bon marché à base de fer comme transporteur d'oxygène dans la combustion en boucle chimique, Oil Gas Sci. Technol. 66 (2) (2011) 235–248, https://doi.org/10.2516/ogst/2010030.
[21] F.J. Velasco-Sarria, C.R. Forero, I. Adánez-Rubio, A. Abad, J. Adánez, Assessment of low-cost oxygen carrier in South-western Colombia, and its use in the in-situ gasification chemical looping combustion technology, Fuel 218 (November 2017) (2018) 417–424, https://doi.org/10.1016/j.fuel.2017.11.078.
[22] ASTM, D 4179–01 Single Pellet Crush Strength of Formed Catalyst Shapes, 2001.
[23] N. Mohammad Pour, H. Leion, M. Rydén, T. Mattisson, Combined cu/Mn oxides as an oxygen carrier in chemical looping with oxygen uncoupling (CLOU), Energy Fuel 27 (10) (2013) 6031–6039, https://doi.org/10.1021/ef401328u.
[24] T. Mattisson, M. Johansson, A. Lyngfelt, Multicycle reduction and oxidation of different types of iron oxide particles-application to chemical-looping combustion, Energy Fuel 18 (3) (2004) 628–637, https://doi.org/10.1021/ef0301405.
[25] V. Purnomo, F. Hildor, P. Knutsson, H. Leion, Interactions between potassium ashes and oxygen carriers based on natural and waste materials at different initial oxidation states, Greenh. Gases Sci. Technol. 534 (2023) 520–534, https://doi.org/10.1002/ghg.2208.
[26] H. Leion, V. Frick, F. Hildor, Experimental method and setup for laboratory fluidized bed reactor testing, Energies 11 (10) (2018), https://doi.org/10.3390/en11102505.
[27] R. Cocco, Y. Arrington, R. Hays, J. Findlay, S.B.R. Karri, T.M. Knowlton, Jet cup attrition testing, Powder Technol. 200 (3) (2010) 224–233, https://doi.org/10.1016/j.powtec.2010.02.029.
[28] W.T. Sturges, R.M. Harrison, Semi-quantitative x-ray diffraction analysis of size fractionated atmospheric particles, Atmos. Environ. 23 (5) (1989) 1083–1098, https://doi.org/10.1016/0004-6981(89)90309-0.
[29] H. Leion, T. Mattisson, A. Lyngfelt, Use of ores and industrial products as oxygen carriers in chemical-looping combustion, Energy Fuel 23 (4) (2009) 2307–2315, https://doi.org/10.1021/ef8008629.
[30] V. Purnomo, D. Yilmaz, H. Leion, T. Mattisson, Study of defluidization of iron- and manganese-based oxygen carriers under highly reducing conditions in a lab-scale fluidized-bed batch reactor, Fuel Process. Technol. 219 (December 2020) (2021) 106874, https://doi.org/10.1016/j.fuproc.2021.106874.
[31] T. Hatanaka, Y. Yoda, Attrition of ilmenite ore during consecutive redox cycles in chemical looping combustion, Powder Technol. 356 (2019) 974–979, https://doi.org/10.1016/j.powtec.2019.09.028.

[32] N. Berguerand, A. Lyngfelt, The use of petroleum coke as fuel in a 10 kWth chemical-looping combustor, Int. J. Greenh. Gas Control 2 (2) (2008) 169–179, https://doi.org/10.1016/j.ijggc.2007.12.004.
[33] J. Jaseliūnaitė, M. Povilaitis, A. Galdikas, Kinetic modeling of grain boundary diffusion: typical, bi-modal, and semi-lamellar polycrystalline coating morphologies, Coatings 12 (7) (2022), https://doi.org/10.3390/coatings12070992.
[34] I. Staničić, et al., Investigating the interaction between ilmenite and zinc for chemical looping, Energy Fuel (2023), https://doi.org/10.1021/acs.energyfuels.3c01052.
[35] A. Fossdal, et al., Study of dimensional changes during redox cycling of oxygen carrier materials for chemical looping combustion, Energy Fuel 29 (1) (2015) 314–320, https://doi.org/10.1021/ef502004k.
[36] V. Purnomo, I. Staničić, T. Mattisson, M. Ryden, H. Leion, Performance of iron sand as an oxygen carrier at high reduction degrees and its potential use for chemical looping gasification, Fuel 339 (2023), https://doi.org/10.1016/j.fuel.2022.127310.
[37] S. Sundqvist, M. Arjmand, T. Mattisson, M. Rydén, A. Lyngfelt, Screening of different manganese ores for chemical-looping combustion (CLC) and chemical-looping with oxygen uncoupling (CLOU), Int. J. Greenh. Gas Control 43 (2015) 179–188, https://doi.org/10.1016/j.ijggc.2015.10.027.
[38] F. Hildor, H. Leion, T. Mattisson, Steel converter slag as an oxygen carrier—interaction with sulfur dioxide, Energies 15 (16) (2022) 1–29, https://doi.org/10.3390/en15165922.
[39] P. Moldenhauer, M. Rydén, T. Mattisson, A. Lyngfelt, Chemical-looping combustion and chemical-looping with oxygen uncoupling of kerosene with Mn- and cu-based oxygen carriers in a circulating fluidized-bed 300 W laboratory reactor, Fuel Process. Technol. 104 (2012) 378–389, https://doi.org/10.1016/j.fuproc.2012.06.013.
[40] Y. Ma, et al., Hierarchical nature of hydrogen-based direct reduction of iron oxides, Scr. Mater. 213 (2022) 114571, https://doi.org/10.1016/j.scriptamat.2022.114571.
[41] H.M. Feilen, Attrition Rate of Oxygen Carriers in Chemical Looping Combustion Systems, University of North Dakota, 2015.
[42] R. Faust, I. Lamarca, A. Schaefer, F. Lind, P. Knutsson, Magnetic properties of ilmenite used for oxygen carrier aided combustion, Fuel 340 (September 2022) (2023) 127593, https://doi.org/10.1016/j.fuel.2023.127593.
[43] T. Sjafrizal, A. Dehghan-Manshadi, D. Kent, M. Yan, M.S. Dargusch, Effect of Fe addition on properties of Ti–6Al-xFe manufactured by blended elemental process, J. Mech. Behav. Biomed. Mater. 102 (May 2019) (2020) 103518, https://doi.org/10.1016/j.jmbbm.2019.103518.
[44] P.G. Esteban, E.M. Ruiz-Navas, E. Gordo, Influence of Fe content and particle size the on the processing and mechanical properties of low-cost Ti-xFe alloys, Mater. Sci. Eng. A 527 (21–22) (2010) 5664–5669, https://doi.org/10.1016/j.msea.2010.05.026.
[45] S. Kr Bhattacharya, et al., Mechanical properties of Fe rich Fe-Si alloys: ab initio local bulk-modulus viewpoint, Mater. Res. Express 4 (11) (2017), https://doi.org/10.1088/2053-1591/aa97a4.
[46] K. Jothimurugesan, J.G. Goodwin, S.K. Gangwal, J.J. Spivey, Development of Fe Fischer-Tropsch catalysts for slurry bubble column reactors, Catal. Today 58 (4) (2000) 335–344, https://doi.org/10.1016/S0920-5861(00)00266-2.
[47] P. Cho, T. Mattisson, A. Lyngfelt, Comparison of iron-, nickel-, copper- and manganese-based oxygen carriers for chemical-looping combustion, Fuel 83 (9) (2004) 1215–1225, https://doi.org/10.1016/j.fuel.2003.11.013.
[48] Y. Xiao, M. Meng, A. Daouadji, Q. Chen, Z. Wu, X. Jiang, Effects of particle size on crushing and deformation behaviors of rockfill materials, Geosci. Front. 11 (2) (2020) 375–388, https://doi.org/10.1016/j.gsf.2018.10.010.
[49] J. Manso, J. Marcelino, L. Caldeira, Single-particle crushing strength under different relative humidity conditions, Acta Geotech. 16 (3) (2021) 749–761, https://doi.org/10.1007/s11440-020-01065-w.
[50] C. Linderholm, P. Knutsson, M. Schmitz, P. Markström, A. Lyngfelt, Material balances of carbon, sulfur, nitrogen and ilmenite in a 100kW CLC reactor system, Int. J. Greenh. Gas Control 27 (2014) 188–202, https://doi.org/10.1016/j.ijggc.2014.05.001.
[51] D. Mei, A.H. Soleimanisalim, C. Linderholm, A. Lyngfelt, T. Mattisson, Reactivity and lifetime assessment of an oxygen releasable manganese ore with biomass fuels in a 10 kWth pilot rig for chemical looping combustion, Fuel Process. Technol. 215 (2021) 106743, https://doi.org/10.1016/j.fuproc.2021.106743.